IJMMM International Journal of Minerals, Metallurgy and Materials 矿物冶金与材料学报（英文版）

Intermetallic growth behavior during post deformation annealing in multilayer Ti/Al/Nb composite interfaces

R. Jafari and B. Eghbali

Cite this article as:
R. Jafari and B. Eghbali, Intermetallic growth behavior during post deformation annealing in multilayer Ti/Al/Nb composite interfaces, *Int. J. Miner. Metall. Mater.*, 29(2022), No. 8, pp. 1608-1617. https://doi.org/10.1007/s12613-021-2263-9

International Journal of Minerals, Metallurgy and Materials
Volume 29, Number 8, August 2022, Page 1608
https://doi.org/10.1007/s12613-021-2263-9

Intermetallic growth behavior during post deformation annealing in multilayer Ti/Al/Nb composite interfaces

R. Jafari[1)] *and B. Eghbali*[2),✉]

1) Department of Materials Engineering, Faculty of Engineering, Urmia University, P.O. Box 57561-165, Urmia, Iran
2) Faculty of Materials Engineering, Sahand University of Technology, P.O. Box 51335-1996, Tabriz, Iran
(Received: 5 August 2020; revised: 20 January 2021; accepted: 26 January 2021)

Abstract: The tri-metal Ti–Al–Nb composites were processed through three procedures: hot pressing, rolling, and hot pressing, followed by subsequent rolling. The fabricated composites were then subjected to annealing at 600, 625, and 650°C temperatures at different times. Microstructure observation at the interfaces reveals that the increase in plastic deformation strain significantly affects $TiAl_3$ intermetallic layers' evolution and accelerates the layers' growth. On the contrary, the amount of applied strain does not significantly affect the evolution of the $NbAl_3$ intermetallic layer thickness. It was also found that Al and Ti atoms' diffusion has occurred throughout the $TiAl_3$ layer, but only Al atoms diffuse through the $NbAl_3$ layer. The slow growth rate of the $NbAl_3$ intermetallic layer is due to the lack of diffusion of Nb atoms and the high activation energy of Al atoms' reaction with Nb atoms.

Keywords: intermetallic compounds; diffusion; Ti/Al/Nb composite; deformation; annealing

1. Introduction

Some applications of laminated composites are in structural, aircraft, and automobile industries because of their low density, excellent mechanical properties, and their moderate price [1–3]. In contrast, Ti/Al composites combined with subsequent proper annealing have potential applications for the economical production of γ-TiAl sheets and metal-intermetallic laminated composites (such as Ti/$TiAl_3$ composite) [4–5]. Some conventional routes for the production of TiAl sheets, such as powder metallurgy [6], near-net-shape casting from high temperatures [6], and hot-pack rolling rout [7], have series of post processing steps like hot pressing, annealing, and hot working that lead to increases in their costs [8]. Besides, because of its low toughness at room temperature, the widespread applications of TiAl are limited in some functions [9].

One of the most effective toughening strategies is the Nb's addition as a ternary element that increases the room temperature ductility and improves the oxidation resistance of TiAl alloys [10]. So far, the Acoff group suggested a method for the fabrication of Nb containing TiAl alloys [11–12]. This technology is based on rolling processing combined with two-stage heat treatment, which develops titanium aluminides [13]. The first stage's temperature is selected below the melting point of Al (~660°C) so that the $TiAl_3$ and $NbAl_3$ intermetallic compounds form in the Ti/Al and Nb/Al interfaces, respectively.

At the second stage, the $TiAl_3$, $NbAl_3$, Nb, and Ti react together at high temperature (~1200°C), and Nb containing TiAl alloy forms. In some other studies, the Ti/Al/Nb composites have been fabricated by only hot rolling [14–15] or hot pressing [16]. As far as Yu *et al.* [17] have concluded, rolling has a positive effect on the mechanical properties of Ti/Al composite, and Tochaee *et al.* [18] and Shaat *et al.* [19] have succeeded to increase the fracture toughness of multilayered composites such as Ti/Al by refining its grains. However, no study was conducted on the comparison of these methods. Also, because of limited research on Nb/Al multilayered composites [20–22], the current understanding of microstructure evolution and diffusion process at the Nb/Al interface is very little. Several studies have experimented with the Ti/Al diffusion couples [5,23–26]. The experiments conducted by Van Loo and Rieck [27] suggest that Al is the only diffusing component, but it was concluded from another study by Luo and Acoff [28] that the diffusion of Ti atoms to the Al side is much more than the diffusion of Al atoms to the Ti side. Moreover, it was illustrated by Xu *et al.* [23] that both Ti and Al are diffused, and most of the growth has happened at the $TiAl_3$/Al interface. It indicates some ambiguity about the mechanism of compound formation in the Ti/Al interface. Accordingly, in the present research, laminated Ti/ Nb/Al diffusion couples were prepared through three procedures, and the influence of the fabrication method on the growth rate of layers in the first annealing stage was investigated. Also, diffusion processes and growth

✉ Corresponding author: B. Eghbali E-mail: eghbali@sut.ac.ir

features of intermetallic layers at each Ti/Al and Nb/Al interface and the intermetallic layers' growth kinetics for both interfaces were studied.

2. Experimental

In the present investigation, two titanium (99.5wt%, 1 mm thickness), two aluminum (99.5wt%, 0.7 mm thickness), and one niobium (99.8wt%, 0.45 mm thickness) elemental sheets were used as starting materials. The chemical compositions of all are shown in Tables 1–3. Dimensions of the sheets were 50 mm × 150 mm cut from the cold-rolled sheets parallel to the initial rolling direction. The surfaces of all sheets were roughened using a steel-wire brush and cleaned ultrasonically in acetone. The prepared sheets were then stacked over each other, and the stacked laminates of Ti, Al, and Nb layers were subjected to hot pressing at 600°C for 1 h under 50 MPa pressure. One of the samples was put aside at this stage (sample 1), and the rest were rolled immediately with thickness reductions of 17% (sample 2), 52% (sample 3), and 77% (sample 4) on a laboratory rolling mill without lubrication at a speed of 3.14 rad/s with rolls of 350 and 450 mm in diameter and length, respectively. After surface treatment and stacking, another sample was processed using the cold rolling method with 65% thickness reductions (sample 5) for comparison. To anneal the fabricated composites, they were cut to the dimension of 10 mm × 6 mm and put in an evacuated and sealed glass capsule. Then, annealing treatments were performed at 600, 625, and 650°C with diffusion times of 30 to 480 min.

Table 1. Composition of the Nb sheet used in this study wt%

Fe	Al	Mg	Nb
0.05	0.07	0.08	99.8

Table 2. Composition of the Ti sheet used in this study wt%

Fe	H	C	N	O	Ti
0.2	0.015	0.08	0.03	0.18	99.62

Table 3. Composition of the Al sheet used in this study wt%

Zn	V	Si	Sb	Pb	Mn	Mg	Fe	Cu	Cr	B	Al
0.055	0.040	0.062	0.062	0.009	0.025	0.025	0.189	0.030	0.007	0.007	99.452

The scanning electron microscope (SEM) equipped with energy dispersive spectroscopy (EDS) was used to characterize new phases. Also, X-ray diffraction analysis (XRD, Cu target, 40 kV, and 40 mA) and transmission electron microscopy (TEM) were conducted to investigate the resultant intermetallic compounds.

TEM sample was prepared by focused ion beam (FIB) method as thin specimens. Electron backscatter diffraction (EBSD) analysis was conducted to characterize the interfacial Ti/Al features. Then, the sample was mounted, carefully ground, and polished. The $TiAl_3$ tetragonal crystal structure with space group $I4/mmm$ and lattice parameters: $a = b =$ 0.38537 nm, $c = 0.85839$ nm, and $\alpha = \beta = \gamma = 90°$ [29] was employed for EBSD analyses, and the data were collected by an SEM equipped with an EBSD analysis system from the selected area with a step size of 0.65 µm. The hardness measurements were carried out at room temperature on samples without annealing, and after annealing, they were done with a Vickers indenter and an applied load of 1 N for 10 s. The measurements were obtained from 3 to 5 indentations. To adjust the intermetallic thickness determination statistics at Ti/Al and Nb/Al interfaces, microstructural image processing (MIP) software was used to measure the width of the intermetallic layers.

3. Results and discussion

3.1. Formation of intermetallic compounds during hot pressing and rolling

The SEM micrographs from Ti/Al and Nb/Al interfaces after pressing are shown in Fig. 1.

As can be seen, intermetallic compounds with low thickness are formed at Ti/Al layers during pressing (Fig. 1 (a)). It is related to the high temperature (600°C) and enough time (60 min) to form intermetallic compounds during hot pressing. The EDS analysis results demonstrate that Al and Ti's atomic concentrations are 76.8at% and 23.2at%, respectively (insert in Fig. 1(a)), which confirms $TiAl_3$ intermetallic compound formation. However, there is no evidence for the formation of the intermetallic layer in the Nb/Al interface (Fig. 1(b)). The EDS line scan analysis across the Nb/Al interface can be seen in insert in Fig. 1(b). It confirms Nb and Al atoms' interdiffusion during pressing, but intermetallic phases could not be detected.

The microstructures and EDS results of sample 1 immediately after pressing and samples 2–5 after rolling are illustrated in Fig. 2. As can be seen, Ti/Al and Nb/Al interfaces are smooth, and no delamination or defect can be observed.

3.2. Microstructural evolutions during post deformation annealing

Microstructural evolutions of samples 1–5 after annealing at 625°C for 480 min are illustrated in Figs. 3 and 4. As observed, the thickness of the $TiAl_3$ intermetallic layer is increased with the increase of rolling reduction (Fig. 3(a)–(e)), but the thickness of the intermetallic layer formed at Nb/Al interface (Fig. 4(a)–(d)) in samples 1–4, is almost constant (~2 µm).

The intermetallic layer thickness in sample 5 at Nb/Al interface is lower (~ 0.5 µm) than the thickness developed during fabrication by pressing. The EDS analysis (Fig. 4(f)) from the intermetallic layer at the Nb/Al interface indicates

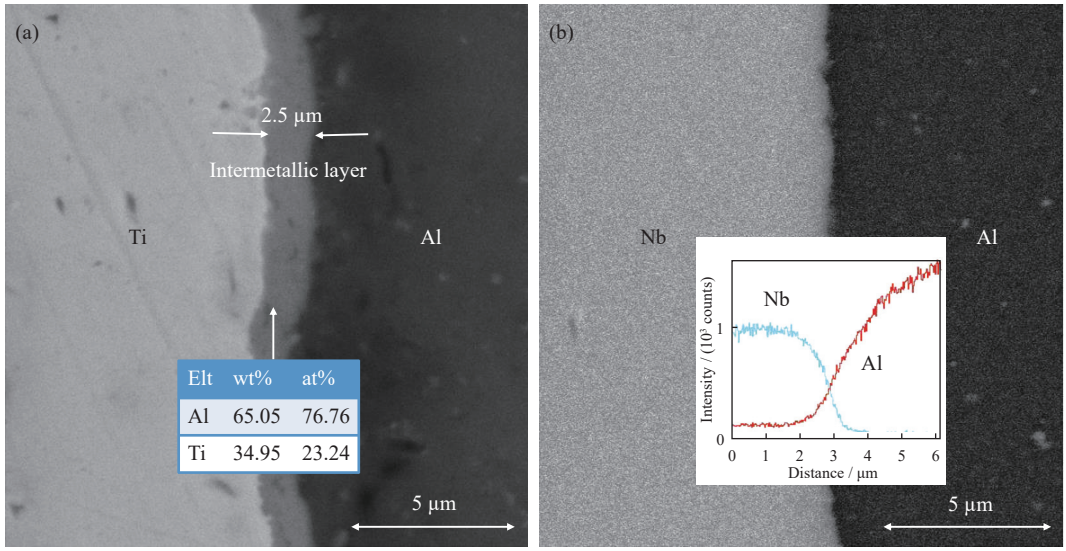

Fig. 1. (a) BSE image of Ti/Al interface and EDS result of the developed layer (Elt—Element) and (b) BSE image of Nb/Al interface and EDS line scan of Nb, Al across the interface at Ti/Al/Nb laminated composite fabricated by hot pressing.

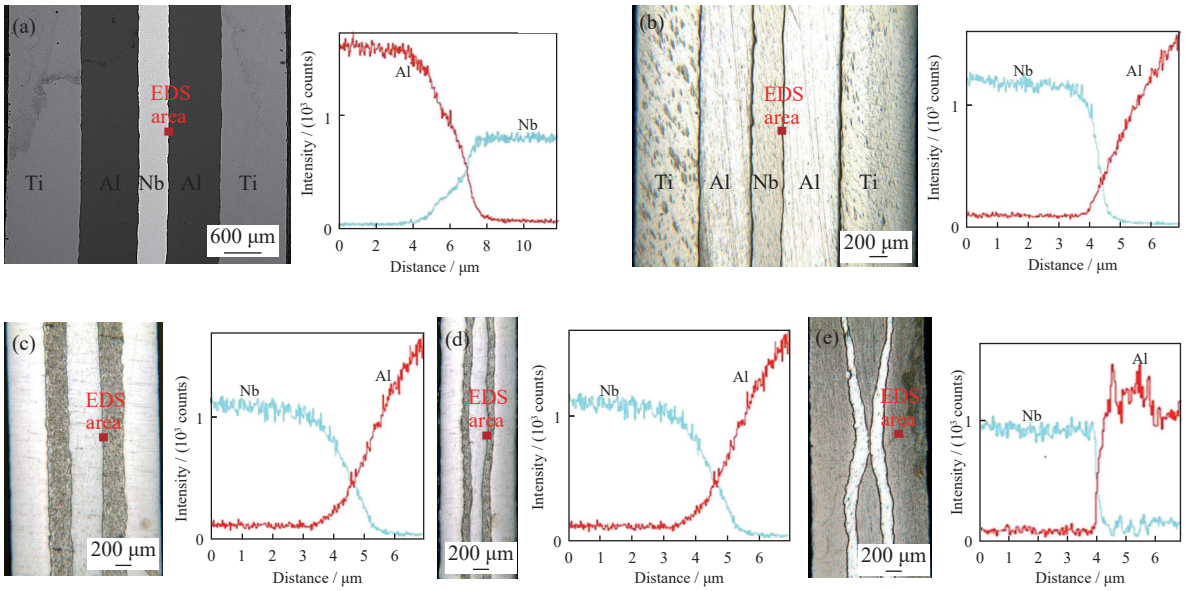

Fig. 2. Microstructures and EDS results of Ti/Al/Nb samples: (a) sample 1 fabricated by hot pressing; (b) sample 2 fabricated by hot pressing followed by 17% reduction; (c) sample 3 fabricated by hot pressing followed by 52% reduction; (d) sample 4 fabricated by hot pressing followed by 77% reduction; (e) sample 5 fabricated by cold rolling ((a) SEM micrograph and (b–e) OM micrographs).

that Al and Nb's atomic concentrations are 77at% and 23at%, respectively. It approves the formation of the $NbAl_3$ intermetallic compound.

According to the mechanism suggested for joining metals during pressing [30], the oxide layers formed on Ti's surface, Al, and Nb's layers are broken during pressing. Then, the Ti/Al and Nb/Al interdiffusion occurred, and diffusion bonding was achieved. Due to Ti's lower melting point and its rapid diffusion compared to Nb, the solid solution formed at Ti/Al interface is saturated, and $TiAl_3$ intermetallic compounds will be developed. Nevertheless, the Nb diffusion rate is slower at the Nb/Al interface due to the higher melting temperature [31]. Thus, the Nb/Al solid solution is not saturated, and the intermetallic compound will not be formed. The $TiAl_3$ intermetallic layer formed in the pressing step is much more brittle. This layer is fractured during the rolling process so that the substrate virgin metals are extruded throughout the initiated cracks and reached together. Therefore, the interface consists of impurity-free Ti/Al contact surface and the fragmented $TiAl_3$ intermetallic compounds, and strain induced interdiffusion occurs according to Ma *et al.* [32]. However, in the Nb/Al interface, a diffusion layer exists (Fig. 2(a)–(d)), which forms during hot pressing, so intermetallic phases are not formed. The diffusion layer's nature is a metallic solid solution and is not brittle as intermetallic compounds. Therefore, the diffusion layer is not fractured as intermetallic compounds. It is expected that the interdiffusions of Al and Ti become more and as a result, the nucleation and

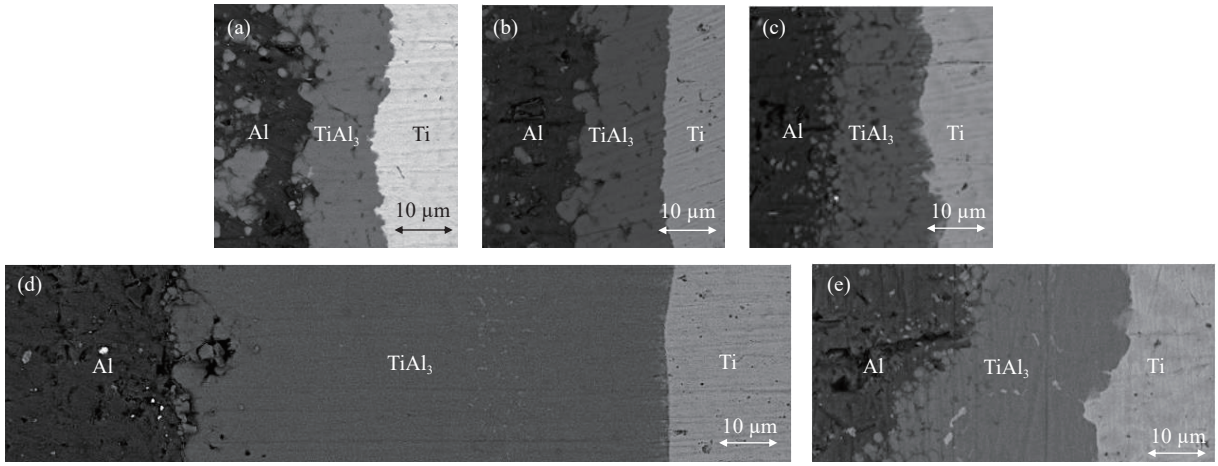

Fig. 3. SEM micrographs of Ti/Al interface of samples 1 (a), 2 (b), 3 (c), 4 (d), and 5 (e) after annealing at 650°C for 480 min (The gray islands in the Al layer is $TiAl_3$, confirming the diffusion of Ti atoms).

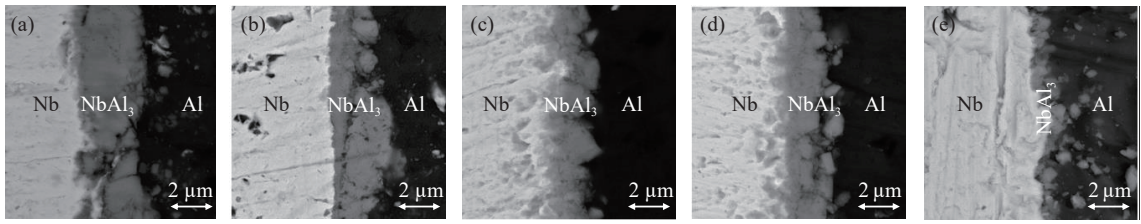

(f)

Elt	wt%	at%
Al	49.52	77.16
Nb	50.48	22.84

Fig. 4. SEM micrographs of Nb/Al interface at samples 1 (a), 2 (b), 3 (c), 4 (d), and 5 (e) after annealing at 650°C for 480 min and (f) EDS result of the developed layer.

growth of the intermetallic layer become easier with increasing plastic strain. It results in the more rapid growth of $TiAl_3$ at higher rolling strains. The intermetallic layer's thickness at the Nb/Al interface in the cold-rolled sample after annealing is very low, illustrating the effect of the Nb/Al diffusion layer formed in high-temperature conditions of pressing on the growth of the intermetallic layer. This diffusion layer makes intermetallic nucleation easy. The intermetallic layer's thickness formed at the Nb/Al interface in sample 5 is very low because the diffusion layer is not formed during cold rolling (Fig. 2(e)). At the highest annealing time, holes will be formed in Al side regions as reported [15]. The main reason for the formation of cavities in Figs. 3 and 4 is related to the difference between the volume of raw materials and the final intermetallic phases' volume. The proposed solution to eliminate these porosities is to apply pressure during annealing [33]. Also, the formation of cracks in intermetallic compounds can be attributed to the brittleness of the intermetallic compounds that may form during the sample preparation process. The results of the XRD analysis of samples annealed at three different temperatures (600, 625, and 650°C) for 480 min is illustrated in Fig. 5. There are peaks of Ti, Nb, Al, and peaks of intermetallic compounds ($TiAl_3$ and $NbAl_3$) at all annealing temperatures. To improve signals of intermetallic compounds, micro-area XRD was performed from $TiAl_3$/Al/ $NbAl_3$ cross-section of a sample annealed at 700°C for 4 h, which is presented in Fig. 6. Therefore, the XRD results confirm the EDS analysis. The results demonstrate the formation of $TiAl_3$ and $NbAl_3$ compounds at Ti/Al/Nb trimetal composite.

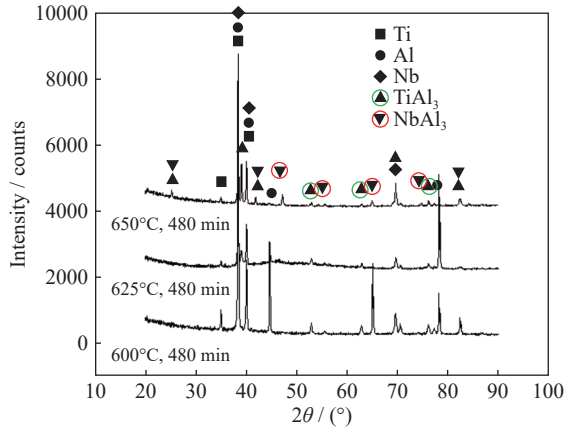

Fig. 5. XRD patterns of Ti/Al/Nb samples after annealing at 600, 625 and 650°C for 480 min (sample 4).

3.3. EBSD and TEM analyses of intermetallic layers

EBSD analysis was performed on the $TiAl_3$ intermetallic layer formed after annealing at 650°C for 480 min, related to sample 4. The results are presented in Fig. 7. It is evident that the intermetallic layer's grain size is adequate at Al/$TiAl_3$ and Ti/$TiAl_3$ interfacial sides. However, the grain structure is coarse at central regions of the $TiAl_3$ intermetallic compound.

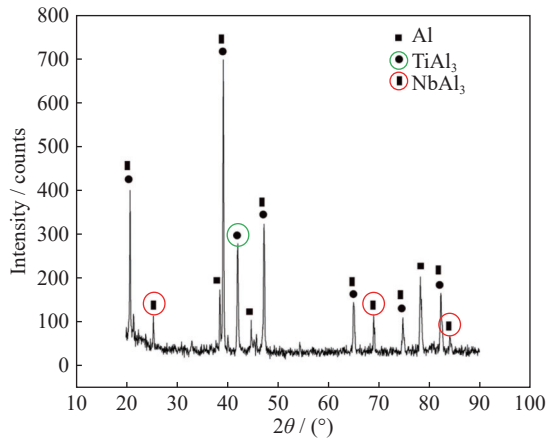

Fig. 6. Micro-area XRD results from $TiAl_3$/Al/$NbAl_3$ cross-section of a sample annealed at 700°C for 4 h (sample 4).

It can be concluded that Ti and Al both diffuse through the intermetallic layer, and $TiAl_3$ nuclei are formed at both of Al/$TiAl_3$ and Ti/$TiAl_3$ interfaces while central grains grow and coarsen during annealing. The presence of more fine grains at the Ti/$TiAl_3$ interface demonstrates rapid diffusion of Al compared with Ti atoms. This result agrees with some previous works suggesting that aluminum is the dominant diffusing element in the Ti–Al couple [34–35]. The black zones through the intermetallic layer are residual Al. This residual Al has been reported by Mirjalili *et al.* [36]. They observed the concentration of Al in $TiAl_3$ grain boundaries after annealing at 650°C for 48 h. Residual Al's existence demonstrates that the nucleation of $TiAl_3$ has not occurred at the Ti/Al interfacial line, but it has occurred in a region. It is deduced that $TiAl_3$ nucleation and growth happen in a region, and a two-phase ($TiAl_3$ + Al) region will be formed. As the annealing is progressed, the amount of Al is reduced. Fig. 7(b) provides the pole figures of the $TiAl_3$ grains formed at the Ti/Al interface at 650°C. As can be seen, the maximum peak intensity is about 1.6 R, demonstrating a very weak texture in the intermetallic layer.

TEM bright-field images of the Nb/Al interface after annealing at 650°C for 480 min (sample 4) are shown in Fig. 8. The location and the photograph of the film prepared by FIB are represented in Fig. 8(a) and (b), respectively. The EDS results from the three points (indicated in Fig. 8(c)) confirm the formation of the $NbAl_3$ intermetallic compound at the interface (Fig. 8(d)). Bright-field TEM image (Fig. 8(c)) illustrates that the Nb/$NbAl_3$ interface is smooth, and Al/Nb Al_3 interface is rough and rugged. The new $NbAl_3$ nuclei are formed near the Nb/$NbAl_3$ interface, and consequently, the smooth interface will appear near the Nb layer. Coarse grains are observed at Al/$NbAl_3$ interface, and fine grains are observed at the Nb/$NbAl_3$ interface. This phenomenon indicates that only Al atoms diffuse, while Nb atoms do not diffuse substantially during annealing. Thus, initially formed grains at the A/$NbAl_3$ begin to grow, and new grains will be formed at the Nb/$NbAl_3$ interface.

3.4. Morphology evolution and formation kinetics of intermetallic compounds during post deformation annealing

The evolution of the intermetallic particle morphology during post deformation annealing is shown in Fig. 9. As mentioned above, the intermetallic particles formed during the pressing stage are fractured during subsequent rolling (Fig. 9(a)), indicated by arrows.

When they grow during annealing, their morphology is changed. The shape of stable nuclei is determined by the particle's surface energy and volume Gibbs free energy [37]. The intermetallic growth in the Al layer indicated that the Al/$TiAl_3$ interface's surface energy is lower than the surface energy of Ti/$TiAl_3$. The particles should have the lowest sur-

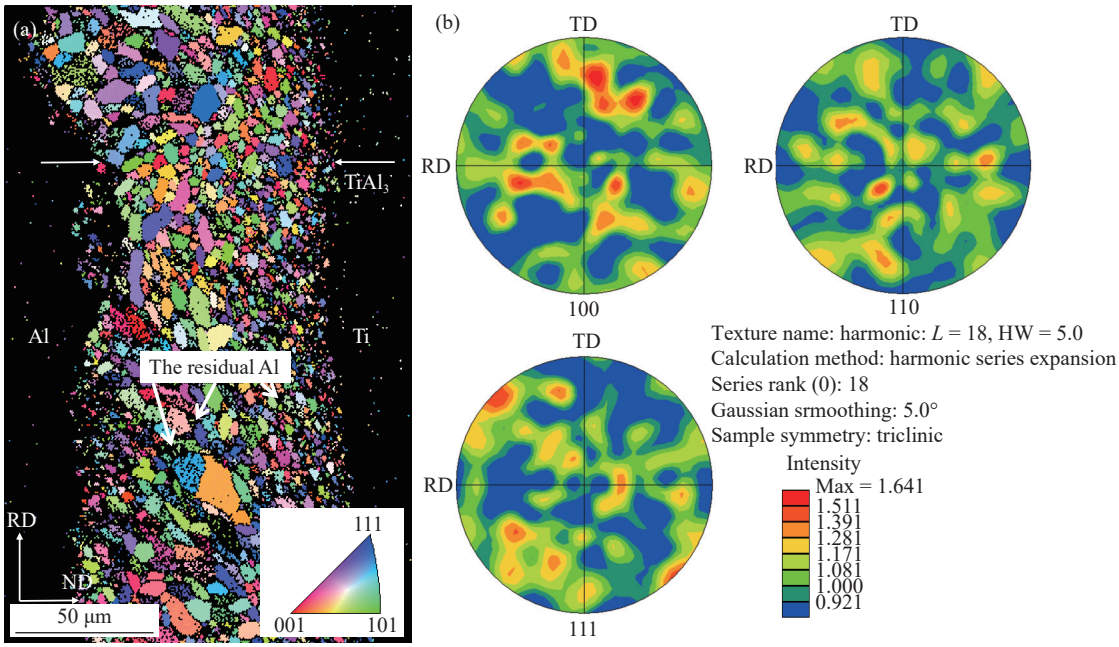

Fig. 7. (a) SEM image and (b) EBSD micrographs from the Ti/Al interface of Ti/Al/Nb laminated composite annealed at 650°C for 480 min (RD—Rolling direction; TD— Transverse direction).

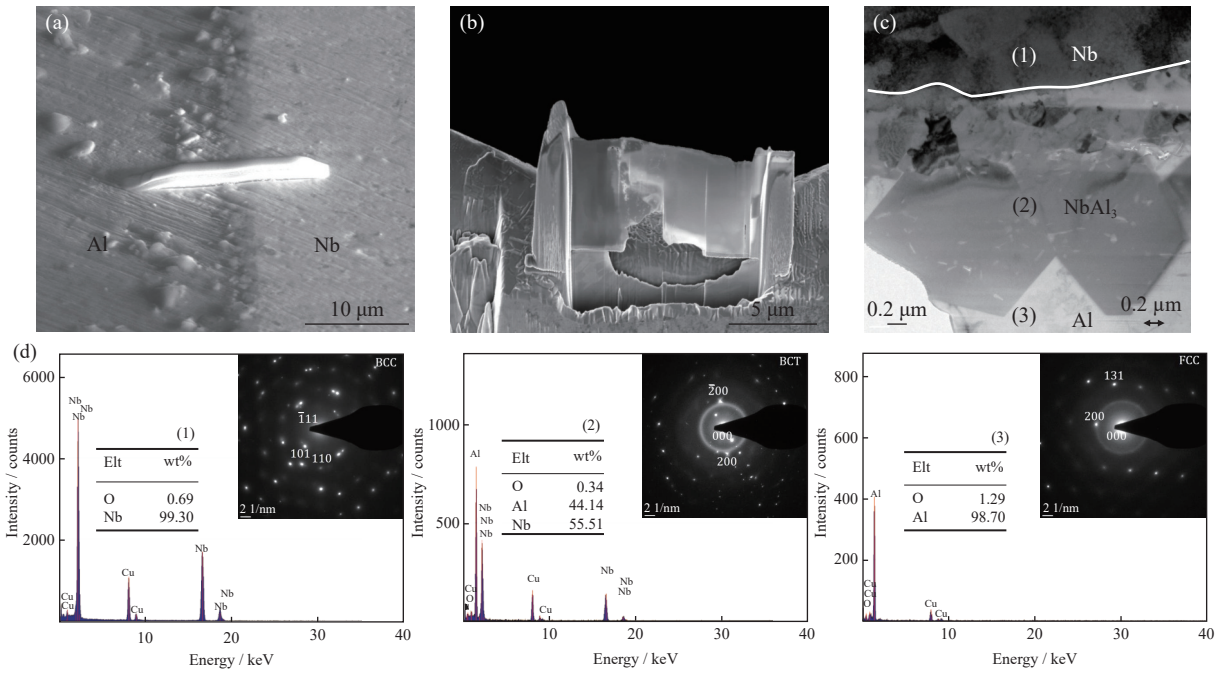

Fig. 8. TEM results from Nb/Al interface of Ti/Al/Nb laminated composite annealed at 650°C for 480 min: (a) the location of the platinum deposited layer; (b) prepared film by FIB method; (c) bright field image of the Nb/Al interface; (d) TEM EDS and SADP results of the points shown in (c).

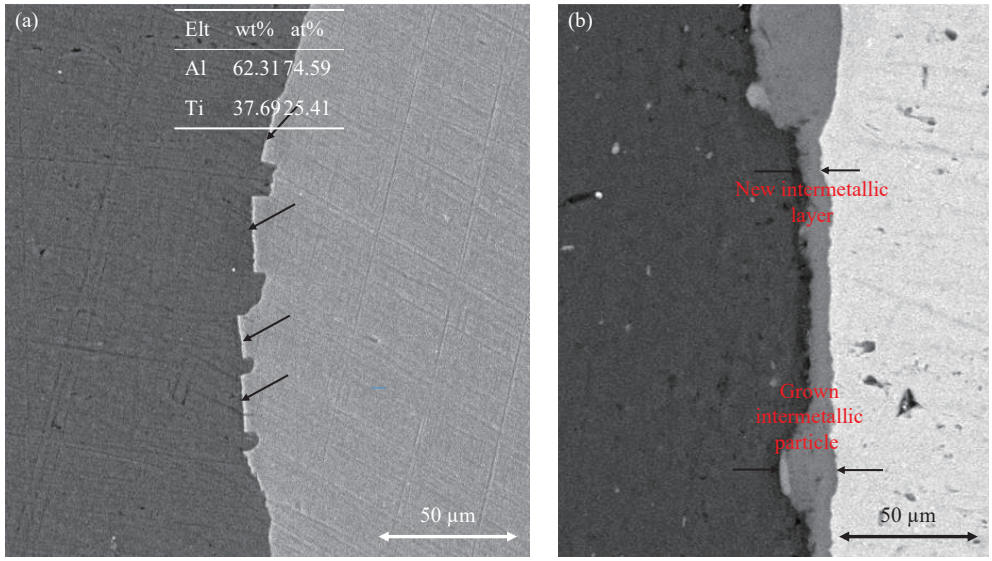

Fig. 9. (a) Ti/Al interface after fabrication by press and subsequent rolling process related to samples 1 (arrows indicating formed intermetallic layers which are fragmented during rolling process) with an EDS result of the white layer; (b) growth of the fragmented particles and uniform intermetallic layer formed at Ti/Al interface during annealing (it is necessary to mention that only the uniform thickness of layers was used for obtaining kinetics data).

face energy so that their shape can be transformed from cubic (Fig. 9(a)) to spherical form (Fig. 9(b)).

The variations of the intermetallic layer's thickness in Ti/Al and Nb/Al interfaces with annealing time and temperature are represented in Figs. 10 and 11, respectively. As seen, the thickness of both intermetallic layers increases with the increase of annealing time and temperature. It is deduced from the comparison of $TiAl_3$ and $NbAl_3$ layer thicknesses that annealing time and temperature affect the growth of $TiAl_3$ more than the growth of the $NbAl_3$ layer.

Thermodynamics and kinetics of the intermetallic phase formation are varied in different studies because of the difference in Ti's chemical composition and especially Al Percentage. Even the oxide layer of the surface affects the kinetics of intermetallic formation.

In the present study, the oxide layer does not exist at the Ti/Al interface because a thin layer of $TiAl_3$ is formed during hot pressing. The intermetallic layer was fragmented during rolling, and virgin metals contact each other in an oxide-free surface, but Nb's oxide layer does not seem to be fractured completely. The present study findings indicate that annealing at 600–650°C temperature range results in the formation

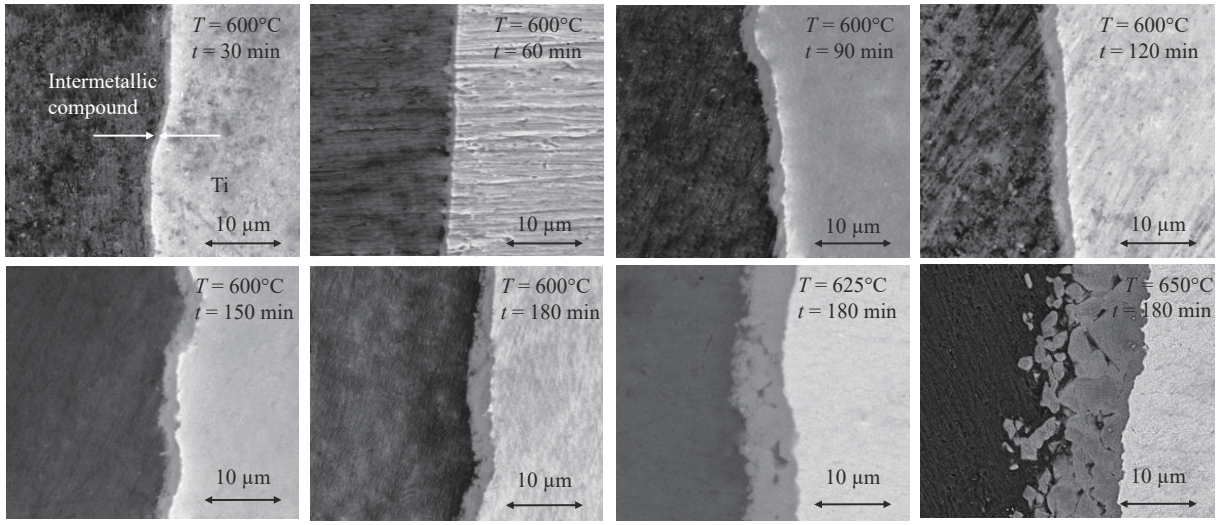

Fig. 10. Effect of annealing time (t) and temperature (T) on the growth of the $TiAl_3$ intermetallic layer.

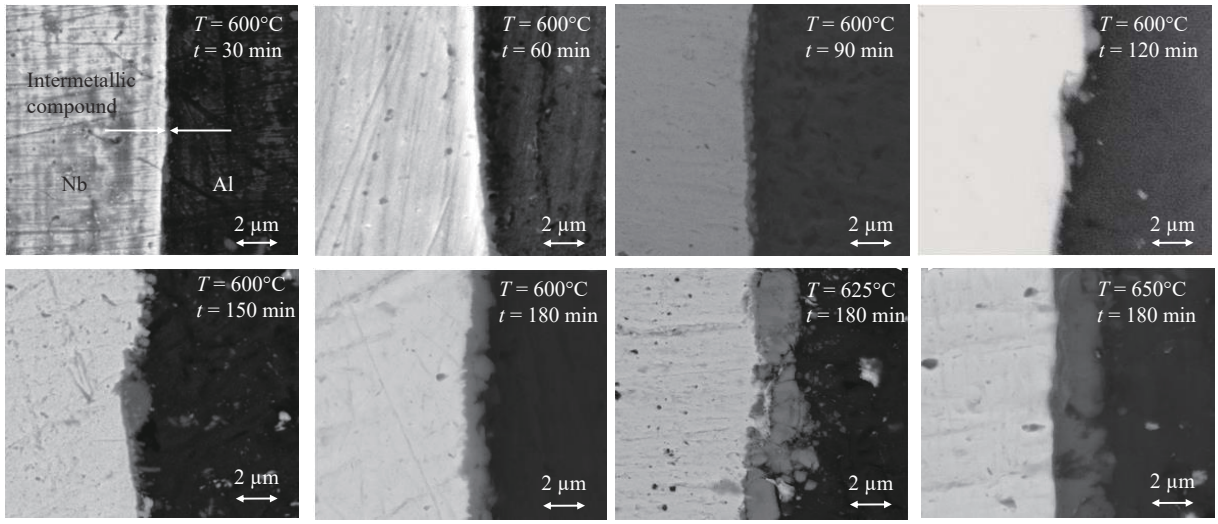

Fig. 11. Effect of annealing time and temperature on the growth of the $NbAl_3$ intermetallic layer.

of $TiAl_3$ and $NbAl_3$ (Figs. 1, 4, and 5) at Ti/Al and Nb/Al interfaces, respectively. However, there are other intermetallic compounds such as $TiAl_2$, TiAl, and Ti_3Al at the Ti/Al equilibrium phase diagram [38]. Other intermetallic compounds of Nb_3Al and Nb_2Al exist at the Nb/Al equilibrium binary phase diagram [38]. The solid crystalline structure of $NbAl_3$ is ordered in the face center tetragonal, and chemical composition changes are narrow around the stoichiometric composition. $NbAl_3$ was reported as the first phase formed at solid Nb/solid Al and solid Nb/liquid Al interfaces in previous studies [20–22]. It was shown that the aluminum concentration at the surface of the niobium and the mechanical properties of the metal are the two factors determining the structure and thickness of the niobium aluminide layers [31]. The reaction rate between Al and Nb is slow due to stable oxide layer formation on the Nb surface. Besides, the activation energy of the reaction of Al and Nb atoms is high. Therefore, the formation of Nb-containing intermetallic compounds is difficult, and the thickness of $NbAl_3$ is lower than the thickness of $TiAl_3$ (Figs. 10 and 11). The absence of other intermetallic compounds is reported by other researchers [26,28,39]. According to some investigations, the absence of other intermetallic compounds is related to the difficulty in the nucleation of these intermetallic phases. However, some other research relates this to the more rapid diffusion of Al in $TiAl_3$ and $NbAl_3$ compared to other phases. Van Loo and Rieck [27] prepared a diffusion couple containing all Al–Ti intermetallic compounds by annealing at 625°C for 15 h. It was observed that other intermetallic layers are disappeared, and only $TiAl_3$ remains.

Therefore, it was concluded that the absence of other intermetallic phases is not related to their nucleation difficulties. It is due to the fast diffusion of Al in $TiAl_3$ and $NbAl_3$ phases.

According to Dybcov [35] theory, if diffusion of one compound (or element) in all of the binary compounds is predominant, only one of the compounds in the binary diagram phase will grow. The melting points of Ti, Al, and Nb are 1670, 660, and 2470°C, respectively. For instance, the annealing temperature of 625°C equals to 0.95 T_m^{Al}, 0.37 T_m^{Ti}, and 0.25 T_m^{Nb} (T_m^{Al}, T_m^{Ti}, and T_m^{Nb} refer to the melting temperature points of Al, Ti, and Nd).

It is expected that the mobility of Al atoms in Ti aluminides and Nb aluminides is more than those of Ti and Nb

atoms. For example, in the Ti–Al diffusion couple, Van Loo and Rieck [27] indicated that the predominant diffusion element is Al, and $TiAl_3$ only grows at interface apart from the melting point, and the radius of diffusing atoms affects their mobility [35]. The atomic radiuses of Ti, Al, and Nb are 0.146, 0.147, and 0.143 nm, respectively, which are almost similar to each other. Thus, Ti and Al atoms diffuse through the $TiAl_3$ interface to the opposite side. All diffusing Al atoms are consumed by Ti and Nb layers for the intermetallic growth. The sufficient diffusion of Ti and Nb atoms is needed to nucleate a new intermetallic phase in Ti/Al and Nb/Al interfaces. The sole presence of $TiAl_3$ and $NbAl_3$ at Ti/Al and Nb/Al interfaces confirms that Al is the predominant diffusing atom. Non-uniform growth of $NbAl_3$ indicates that the growth rate is not similar at different crystallographic directions. Thus, a similar result was not found for $TiAl_3$, and this layer's growth is uniform. As mentioned before, the EBSD and TEM results demonstrate that Ti and Al atoms diffuse through the $TiAl_3$ layer and react with Al and Ti at $Al/TiAl_3$ and $Ti/TiAl_3$ interfaces, respectively. Also, Al atoms diffuse through the $NbAl_3$ layer and react with Nb atoms at $NbAl_3$/Nb interface. The formation of a continuous $TiAl_3$ and $NbAl_3$ layers is followed by reactions (1) (at $Ti/TiAl_3$ interface), (2) (at $Al/TiAl_3$ interface), and (3) (at $Nb/NbAl_3$ interface) as mentioned below (the subscripts of "dif" and "surf" at these equations refer to diffused and surface atoms, respectively).

$$3Al_{dif} + Ti_{surf} = TiAl_3 \quad (1)$$

$$3Al_{surf} + Ti_{dif} = TiAl_3 \quad (2)$$

$$3Al_{dif} + Nb_{surf} = NbAl_3 \quad (3)$$

It should be mentioned that in a heterogeneous system obtained at constant time and temperature, no reaction was happened at $TiAl_3$ and $NbAl_3$ bulk material by assuming Ti and Al as diffusing atoms through $TiAl_3$ and Al atoms diffusing through $NbAl_3$.

The kinetics equation for the growth (dx/dt) of $TiAl_3$ and $NbAl_3$ can be described by Eqs. (4) and (5), respectively

$$\frac{dx}{dt} = \frac{k_{reacAl1}}{1 + \frac{k_{reacAl1}x}{k_{diffAl1}}} + \frac{k_{reacTi2}}{1 + \frac{k_{reacAl1}x}{k_{diffTi2}}} \quad (4)$$

$$\frac{dx}{dt} = \frac{k_{reacAl4}}{1 + \frac{k_{reacAl4}x}{k_{diffAl4}}} \quad (5)$$

where the k_{reac}, k_{diff}, and x refer to reaction constant, diffusion constant, and intermetallic thickness, respectively. Subtitle numbers at these equations point to the position of reactions, which is shown in Fig. 12.

In Eqs. (4) and (5), k_{reac} and k_{diff} are chemical and physical constants. The equations can be simplified according to Table 4, and thereby the amounts of x (or thickness of the intermetallic layers) are relatively high. Eq. (4) can be rewritten as Eq. (6).

$$\frac{dx}{dt} = \frac{k_{diffAl1}}{x} + \frac{k_{diffTi2}}{x} \quad (6)$$

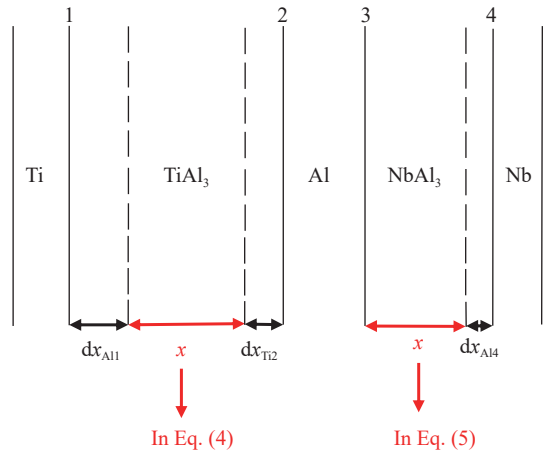

Fig. 12. Schematic for growth of $TiAl_3$ and $NbAl_3$ intermetallic layers at Ti/Al/Nb diffusion couples.

By integration at $t = 0$, $x = 0$ preliminary conditions, the relation between the intermetallic layer's thickness and annealing time can result in a parabolic function (Eq. (7)).

$$x^2 = 2(k_{diffAl1} + k_{diffTi2})t \quad (7)$$

Table 4. Average thickness of $TiAl_3$ and $NbAl_3$ layers at different annealing times and temperatures obtained by MIP software

T / °C	t / min	x / μm	
		$NbAl_3$	$TiAl_3$
600	30	0.25	0.88
	60	0.37	0.96
	150	0.69	2.91
	210	1.05	3.42
	270	1.20	3.51
	300	1.50	4.01
	360	1.86	4.78
	420	1.80	5.10
	480	2.31	7.23
625	30	0.34	1.52
	60	0.46	2.84
	150	0.74	5.83
	210	1.37	7.31
	270	1.72	7.63
	300	1.80	8.51
	360	1.86	11.97
	420	2.46	12.91
	480	2.20	19.85
650	30	0.57	6.82
	60	0.63	8.10
	90	1.03	8.89
	150	1.71	11.91
	210	2.29	13.49
	270	3.60	15.48
	300	3.32	15.49
	360	2.87	16.92
	420	3.38	15.63
	480	6.75	31.83

However, when x values are less than 1, Eq. (5) can be rewritten as Eq. (8). Integration at $t = 0$, $x = 0$ preliminary conditions, the linear relation is obtained between intermetallic layer thickness and annealing time as Eq. (9).

$$\frac{dx}{dt} = k_{reacAl4} \tag{8}$$

$$x = k_{reacAl4} t \tag{9}$$

In Eq. (9), $k_{reacAl4}$ depends on the interface structure, and the interface controls the kinetics of the $NbAl_3$ growth. Plots of the $\ln \Delta x$ versus $\ln t$ for three temperatures obtained using the data shown in Table 4 for $TiAl_3$ and $NbAl_3$ layers are represented in Figs. 13 and 14, respectively. Linear regression analysis for $TiAl_3$ gives straight lines, with values of the kinetic exponent (n) of 0.79, 0.72, and 0.46 at 600, 625 and 650°C, respectively. They are close to 0.5. The kinetic exponent (n) of $NbAl_3$ for the temperatures of 600, 625, and 650°C is 0.83, 0.79, and 0.85, respectively, which are close to 1. It indicates that Eqs. (7) and (9) are appropriate equations to describe $TiAl_3$ and $NbAl_3$ intermetallic layers' growth behaviors, respectively. The $n = 0.5$ suggests that the growth of the $TiAl_3$ layer is controlled by diffusion, and the growth of the NbA_{l3} layer is controlled by interface reaction due to $n = 1$ [39].

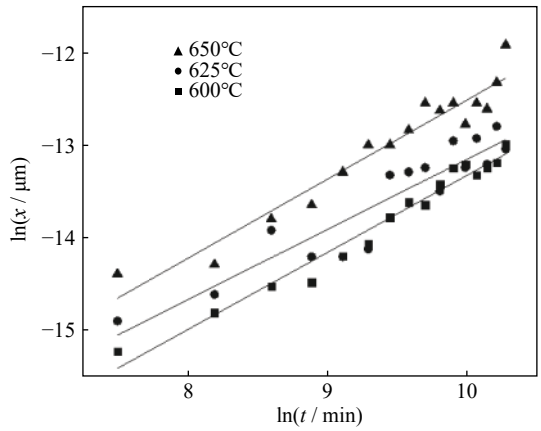

Fig. 13. ln x versus ln t plots for $TiAl_3$ with linear regression at temperatures of 600, 625 and 650°C (the data used for the plot is reported at Table 4).

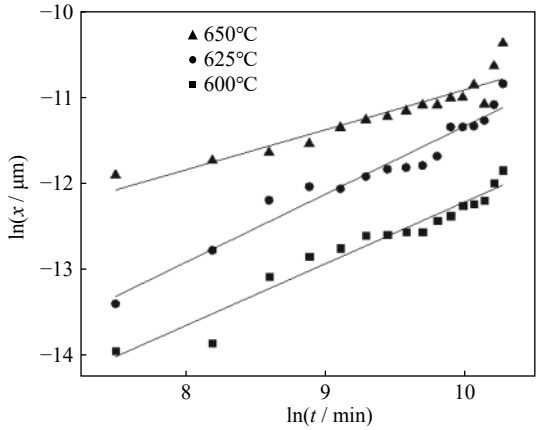

Fig. 14. ln x versus ln t plots for $NbAl_3$ with linear regression at temperatures of 600, 625 and 650°C (the data used for the plot is reported at Table 4).

Gibbs free energies for the formation of $TiAl_3$ and $NbAl_3$ intermetallic compounds are as follows [40–41]:

$$\Delta G_{TiAl_3} = -40349 + 10T,\ \text{J/mol} \tag{10}$$

$$\Delta G_{NbAl_3} = -48350 + 13T,\ \text{J/mol} \tag{11}$$

The variation of Gibbs free energies during the formation of $TiAl_3$ and $NbAl_3$ compounds at 650°C is calculated to be −31 kJ/mol and −36 kJ/mol, respectively. It is indicated that the chemical potential of $NbAl_3$ formation is higher than the chemical potential of $TiAl_3$ formation from a thermodynamics point of view, but according to experiments performed in this research, the formation rate of the $NbAl_3$ layer is very low compared to the formation rate of $TiAl_3$ layer.

4. Conclusions

Systematic research was carried out to process Ti/Al/Nb multilayer composites through different deformation and subsequent annealing procedures in the present research. The processed composites were then subjected to annealing at different temperatures and times. The main results are summarized below.

(1) For the first time, tri-metal Ti/Al/Nb laminated composites were fabricated with good bonding between the layers by hot pressing followed by subsequent rolling.

(2) The increase of the strain in the rolling stage did not significantly affect the growth of the $NbAl_3$ layer. On the contrary, the applied strain has significant effects on the thickness of the $TiAl_3$ intermetallic compound. Therefore, good thicknesses of $TiAl_3$ and $NbAl_3$ layers can be obtained by combining pressing and rolling.

(3) At the Ti/Al interface, both Al and Ti are diffusing elements, but Al is the diffusing element only at the Nb/Al interface. Thus, the equations for describing the intermetallic layers' growth at Ti/Al and Nb/Al layers differ.

(4) The growth of the $TiAl_3$ layer follows the parabolic equation at 600–650°C while the growth of the $NbAl_3$ layer follows linear relation at all annealing temperatures. The $NbAl_3$ intermetallic layer's low thickness is due to the lack of diffusion of Nb atoms and the high activation energy of Al atoms' reaction with Nb atoms.

Acknowledgement

The authors would like to thank Bilkent University for parts of the experiments carried out in the Ulusal Nanoteknoloji Araştırma Merkezi (UNAM) laboratory.

Conflict of Interest

The authors have no affiliation with any organization with a direct or indirect financial interest in the subject matter discussed in the manuscript.

References

[1] A. Patselov, B. Greenberg, S. Gladkovskii, R. Lavrikov, and E.

Borodin, Layered metal-intermetallic composites in Ti–Al system: Strength under static and dynamic load, *AASRI Procedia*, 3(2012), p. 107.
[2] M.S. Abd-Elwahed and A.F. Meselhy, Experimental investigation on the mechanical, structural and thermal properties of Cu–ZrO_2 nanocomposites hybridized by graphene nanoplatelets, *Ceram. Int.*, 46(2020), No. 7, p. 9198.
[3] A.I. Khdair and A. Fathy, Enhanced strength and ductility of Al–SiC nanocomposites synthesized by accumulative roll bonding, *J. Mater. Res. Technol.*, 9(2020), No. 1, p. 478.
[4] J.G. Luo and V.L. Acoff, Processing gamma-based TiAl sheet materials by cyclic cold roll bonding and annealing of elemental titanium and aluminum foils, *Mater. Sci. Eng. A*, 433(2006), No. 1-2, p. 334.
[5] X.P. Cui, G.H. Fan, L. Geng, Y. Wang, H.W. Zhang, and H.X. Peng, Fabrication of fully dense TiAl-based composite sheets with a novel microlaminated microstructure, *Scripta Mater.*, 66(2012), No. 5, p. 276.
[6] Q. Peng, B. Yang, L.B. Liu, C.J. Song, and B. Friedrich, Porous TiAl alloys fabricated by sintering of TiH_2 and Al powder mixtures, *J. Alloys Compd.*, 656(2016), p. 530.
[7] W. Sun, F.H. You, F.T. Kong, X.P. Wang, and Y.Y. Chen, Fracture mechanism of a high tensile strength and fracture toughness Ti6Al4V–TiAl laminated composite, *J. Alloys Compd.*, 820(2020), art. No. 153088.
[8] G.P. Chaudhari and V.L. Acoff, Titanium aluminide sheets made using roll bonding and reaction annealing, *Intermetallics*, 18(2010), No. 4, p. 472.
[9] F. Appel, J.D.H. Paul, P. Staron, M. Oehring, O. Kolednik, J. Predan, and F.D. Fischer, The effect of residual stresses and strain reversal on the fracture toughness of TiAl alloys, *Mater. Sci. Eng. A*, 709(2018), p. 17.
[10] X.F. Ding, J.P. Lin, L.Q. Zhang, Y.Q. Su, and G.L. Chen, Microstructural control of TiAl–Nb alloys by directional solidification, *Acta Mater.*, 60(2012), No. 2, p. 498.
[11] R.G. Zhang and V.L. Acoff, Processing sheet materials by accumulative roll bonding and reaction annealing from Ti/Al/Nb elemental foils, *Mater. Sci. Eng. A*, 463(2007), No. 1-2, p. 67.
[12] X.J. Xu, L.H. Xu, J.P. Lin, Y.L. Wang, Z. Lin, and G.L. Chen, Pilot processing and microstructure control of high Nb containing TiAl alloy, *Intermetallics*, 13(2005), No. 3-4, p. 337.
[13] R. Jafari, B. Eghbali, and M. Adhami, Influence of annealing on the microstructure and mechanical properties of Ti/Al and Ti/Al/Nb laminated composites, *Mater. Chem. Phys.*, 213(2018), p. 313.
[14] Y.Q. Zhao, D. Zhang, Y.B. Sun, Z.J. Wang, R.X. Zheng, and C.L. Ma, Fabrication of TiAlNb alloy sheet by sintering pure metal foils, *Rare Met.*, 30(2011), No. 1, p. 331.
[15] Y.B. Sun, Y.Q. Zhao, D. Zhang, C.Y. Liu, H.Y. Diao, and C.L. Ma, Multilayered Ti–Al intermetallic sheets fabricated by cold rolling and annealing of titanium and aluminum foils, *Trans. Nonferrous Met. Soc. China*, 21(2011), No. 8, p. 1722.
[16] A.M. Patselov, V.V. Rybin, B.A. Grinberg, M.A. Ivanov, and O.V. Eremina, Synthesis and properties of Ti–Al laminated composites with an intermetallic layer, *Russ. Metall.*, 2011(2011), No. 4, p. 356.
[17] H.L. Yu, C. Lu, A.K. Tieu, H.J. Li, A. Godbole, and C. Kong, Annealing effect on microstructure and mechanical properties of Al/Ti/Al laminate sheets, *Mater. Sci. Eng. A*, 660(2016), p. 195.
[18] E. Basiri Tochaee, H.R. Madaah Hosseini, and S.M. Seyed Reihani, Fabrication of high strength *in situ* Al–Al_3Ti nanocomposite by mechanical alloying and hot extrusion: Investigation of fracture toughness, *Mater. Sci. Eng. A*, 658(2016), p. 246.
[19] M. Shaat, A. Fathy, and A. Wagih, Correlation between grain boundary evolution and mechanical properties of ultrafine-grained metals, *Mech. Mater.*, 143(2020), art. No. 103321.
[20] D.S. Chung, M. Enoki, and T. Kishi, Microstructural analysis and mechanical properties of *in situ* Nb/Nb-aluminide layered materials, *Sci. Technol. Adv. Mater.*, 3(2002), No. 2, p. 129.
[21] K.R. Coffey, K. Barmak, D.A. Rudman, and S. Foner, Thin film reaction kinetics of niobium/aluminum multilayers, *J. Appl. Phys.*, 72(1992), No. 4, p. 1341.
[22] G. Lucadamo, K. Barmak, D.T. Carpenter, and J.M. Rickman, Microstructure evolution during solid state reactions of Nb/Al multilayers, *Acta Mater.*, 49(2001), No. 14, p. 2813.
[23] L. Xu, Y.Y. Cui, Y.L. Hao, and R. Yang, Growth of intermetallic layer in multi-laminated Ti/Al diffusion couples, *Mater. Sci. Eng. A*, 435-436(2006), p. 638.
[24] D. Zhang, Y.B. Sun, Y.Q. Zhao, T.T. Wang, J. Chen, H.X. Li, and C.L. Ma, Interfacial products in SiC fiber reinforced Ti–Al based intermetallic alloys, *Rare Met.*, 30(2011), No. 1, p. 524.
[25] H. Wu, G.H. Fan, X.P. Cui, L. Geng, S.H. Qin, and M. Huang, A novel approach to accelerate the reaction between Ti and Al, *Micron*, 56(2014), p. 49.
[26] Y. Mishin and C. Herzig, Diffusion in the Ti–Al system, *Acta Mater.*, 48(2000), No. 3, p. 589.
[27] F.J.J. Van Loo and G.D. Rieck, Diffusion in the titanium-aluminium system—I. Interdiffusion between solid Al and Ti or Ti–Al alloys, *Acta Metall.*, 21(1973), No. 1, p. 61.
[28] J.G. Luo and V.L. Acoff, Interfacial reactions of titanium and aluminum during diffusion welding, *Weld. J.*, 79(2000), No. 9, p. 239.
[29] D.M. Fronczek, J. Wojewoda-Budka, R. Chulist, A. Sypien, A. Korneva, Z. Szulc, N. Schell, and P. Zieba, Structural properties of Ti/Al clads manufactured by explosive welding and annealing, *Mater. Des.*, 91(2016), p. 80.
[30] N. Bay, Mechanisms producing metallic bonds in cold welding, *Weld. J.*, 62(1983), No. 5, p. 137.
[31] G. Slama and A. Vignes, Coating of niobium and niobium alloys with aluminium: Part II. Hot-dipped coatings, *J. Less Common Met.*, 24(1971), No. 1, p. 1.
[32] M. Ma, P. Huo, W.C. Liu, G.J. Wang, and D.M. Wang, Microstructure and mechanical properties of Al/Ti/Al laminated composites prepared by roll bonding, *Mater. Sci. Eng. A*, 636(2015), p. 301.
[33] M. Nofar, H.R. Madaah Hosseini, and N. Kolagar-Daroonkolaie, Fabrication of high wear resistant Al/Al_3Ti metal matrix composite by *in situ* hot press method, *Mater. Des.*, 30(2009), No. 2, p. 280.
[34] D.J. Goda, N.L. Richards, W.F. Caley, and M.C. Chaturvedi, The effect of processing variables on the structure and chemistry of Ti-aluminide based LMCS, *Mater. Sci. Eng. A*, 334(2002), No. 1-2, p. 280.
[35] V.P. Dybkov, *Growth Kinetics of Chemical Compound Layers*, Cambridge International Science Publishing Ltd, 1998.
[36] M. Mirjalili, M. Soltanieh, K. Matsuura, and M. Ohno, On the kinetics of $TiAl_3$ intermetallic layer formation in the titanium and aluminum diffusion couple, *Intermetallics*, 32(2013), p. 297.
[37] X.Y. Liu and P. Bennema, Morphology of crystals: Internal and external controlling factors, *Phys. Rev. B*, 49(1994), No. 2, p. 765.
[38] P. Villars and H. Okamoto, *Al–Nb Binary Phase Diagram 0–100 at.% Nb*, Springer Materials, Japan [2016-06-02]. http://materials.springer.com/isp/phase-diagram/docs/c_0103042
[39] X.P. Cui, G.H. Fan, L. Geng, Y. Wang, L.J. Huang, and H.X. Peng, Growth kinetics of $TiAl_3$ layer in multi-laminated Ti–(TiB_2/Al) composite sheets during annealing treatment, *Mater. Sci. Eng. A*, 539(2012), p. 337.
[40] Y. Nakayama and H. Mabuchi, Formation of ternary L12 compounds in Al_3Ti-base alloys, *Intermetallics*, 1(1993), No. 1, p. 41.
[41] T. Takemoto and I. Okamoto, Intermetallic compounds formed during brazing of titanium with aluminium filler metals, *J. Mater. Sci.*, 23(1988), No. 4, p. 1301.